

State estimation and finite-frequency fault detection for interconnected switched cyber-physical systems

Shenghui GUO¹, Mingzhu TANG¹, Darong HUANG^{2*} & Jiafeng SONG³

¹*School of Electronic and Information Engineering, Suzhou University of Science and Technology, Suzhou 215009, China;*

²*School of Artificial Intelligence, Anhui University, Hefei 230601, China;*

³*Tsinghua University Suzhou Automobile Research Institute, Suzhou 215200, China*

Received 16 October 2022/Revised 2 January 2023/Accepted 6 February 2023/Published online 28 August 2023

Abstract For switched cyber-physical systems with disturbances and actuator faults, we address fault detection and isolation problems. First, the preconditions relative to subsystems are discussed in detail, and the original subsystems are turned into an overall system. Second, the frequency ranges of faults are considered to belong to the finite-frequency domain, and the observer, which makes the residual robust against disturbances and sensitive to faults, is designed by combining the finite-frequency H_- technique with the mixed $L_2 - L_\infty/H_\infty$ technique. Third, design conditions, which guarantee that the error system is stable and satisfies the mixed performance, are derived using the average dwell time method and Lyapunov functionals. Finally, a traffic density dynamic model is proposed to demonstrate the validity and effectiveness of the proposed method.

Keywords switched system, fault detection and isolation, mixed $L_2 - L_\infty/H_\infty$, H_- technique

Citation Guo S H, Tang M Z, Huang D R, et al. State estimation and finite-frequency fault detection for interconnected switched cyber-physical systems. *Sci China Inf Sci*, 2023, 66(9): 192204, <https://doi.org/10.1007/s11432-022-3705-2>

1 Introduction

As a multi-mode system, switched systems' models are dominated by switching signals. In recent decades, it has been confirmed that switched systems are of great importance in various applications, such as aircraft control systems, artificial neural networks, electric systems, and traffic density estimation [1–3].

To guarantee the stability of a system, several methods have been applied in [4–8]. According to the dwell time method, much has been achieved in switched systems [9–12]. Because switched systems contain unstable modes, methods for addressing the stability problem were presented in [13, 14]. The average dwell time (ADT) method was provided in [15–18]. In [17], by considering systems with switching transition rates, sufficient conditions for L_1 -gain performance were provided by combining linear co-positive Lyapunov functions with the ADT method. In [18], the problem of a nonlinear switched system's stability was solved by considering the multiple discontinuous Lyapunov functions and the mode-dependent ADT method.

On another research frontier of switched systems, it is important to design the fault detection and isolation (FDI) method. Several types of results on observer design have been conducted [19–22], and the $L_2 - L_\infty$ performance has been discussed in [23–25]. In [26], considering a switched piecewise-affine system, a filter that is mode-dependent and region-dependent was proposed to guarantee a system's stability, and the finite-time $L_2 - L_\infty$ performance was satisfied. In [27, 28], for switched neural networks, non-fragile $L_2 - L_\infty$ filters were designed using mode-dependent Lyapunov functions, which were subjected to either additive or multiplicative gain perturbations. In [29], the admissible edge-dependent average dwell time switching method was provided, and the $L_2 - L_\infty$ performance was guaranteed by considering Lyapunov functions and unknown disturbances. In practical switched control systems, H_∞ control has shown effectiveness [30–32]. Based on the event-triggered strategy, an H_∞ filter was introduced to address

* Corresponding author (email: drhuangjs@ahu.edu.cn)

the control problem of network switched systems in [33]; H_∞ and $L_2 - L_\infty$ performance was satisfied in [34]. In [35, 36], a robust fault detection observer with an H_∞ index was devised to accomplish fault detection and estimation by comparing generated residuals with the generated threshold. Combining the fault sensitivity with disturbance robustness, H_∞/H_- performance analysis was considered in [37, 38]. In several applications, the $L_2 - L_\infty$ and the H_∞ controls can be considered valuable methods. The preceding literature only considered a single performance index. A helpful method considering the above indexes is to be proposed. Moreover, combining the $L_2 - L_\infty/H_\infty$ performance with the H_- performance and then applying them to FDI for switched systems are important issues. Because of its complexity, the cyber-physical system (CPS) is vulnerable to faults. Most existing methods for interconnected systems suppose that only one subsystem is affected by the fault, which is considered in the full-frequency domain. Among the above literature, the contributions of this paper are summarized as follows.

(1) The proposed method differs from the methods using a single index in [39–41] in that it is designed based on the mixed $L_2 - L_\infty/H_\infty$ performance. Then, the ADT method, which is used to guarantee that the system is stable, is employed to design the switching signal. Therefore, the proposed method combines two indexes in the unified framework, which is more flexible and effective.

(2) Compared with the methods in [37, 42, 43], a detection scheme is provided, where fault signals are considered to belong to a finite-frequency domain in an interconnected CPS using a switching strategy, and sufficient conditions are proposed.

(3) Unlike previously proposed strategies in [36, 44, 45], the finite-frequency H_- performance is additionally constructed considering the fault sensitivity. By considering the generalized Kalman-Yakubovich-Popov Lemma, detection conditions are provided as linear matrix inequalities (LMIs) through additional parameters and matrices.

This paper is structured as follows. Section 2 presents system models and preliminaries. The fault detection scheme and isolation scheme are then introduced in Sections 3 and 4, respectively. Sufficient design conditions are established. Section 5 provides simulations to verify the feasibility of the proposed method. Finally, conclusions are summarized in Section 6.

Notations. For ease of description, the following symbols are defined. \mathbb{R}^n and $\mathbb{R}^{m \times n}$ represent n -dimensional and $m \times n$ dimensional Euclidean spaces, respectively. For a symmetric matrix A , $A > 0$ implies that it is positive definite, and $\lambda_{\min}(A)$ and $\lambda_{\max}(A)$ are the minimum and maximum eigenvalues of A , respectively. The Hermitian part of A is expressed as $\text{He}\{A\} = A + A^T$. The symbol \otimes represents the Kronecker product.

2 System descriptions and preliminaries

N subsystems are in the interconnected CPS with unknown disturbances and faults, and the motion of the t -th subsystem using the switching strategy at moment k is modeled as

$$\begin{cases} x_t(k+1) = A_{t,\sigma(k)}x_t(k) + B_{t,\sigma(k)}u_t(k) + D_{t,\sigma(k)}\eta_t(k) \\ \quad + E_{t,\sigma(k)}f_t(k) - a \sum_{\substack{j=1 \\ j \neq t}}^N g_{tj}\Lambda y_j(k), \\ y_t(k) = C_{t,\sigma(k)}x_t(k), \quad t = 1, \dots, N, \end{cases} \quad (1)$$

where $x_t(k) \in \mathbb{R}^{n_x}$, $u_t(k) \in \mathbb{R}^{n_u}$, $\eta_t(k) \in \mathbb{R}^{n_\eta}$, and $f_t(k) \in \mathbb{R}^{n_f}$ represent the state vector, the control input, the unknown input, and the fault signal, respectively. a denotes the coupling strength, and Λ is the coupling matrix. $\sigma(k) : R^+ \rightarrow \mathcal{L} = \{1, 2, \dots, l\}$ denotes the switching signal. For $k \in [k_s, k_{s+1})$, $\sigma(k) = i$ and k_s is the switching instant. $A_{t,\sigma(k)} \in \mathbb{R}^{n_x \times n_x}$, $B_{t,\sigma(k)} \in \mathbb{R}^{n_x \times n_u}$, $C_{t,\sigma(k)} \in \mathbb{R}^{n_y \times n_x}$, $D_{t,\sigma(k)} \in \mathbb{R}^{n_x \times n_\eta}$, and $E_{t,\sigma(k)} \in \mathbb{R}^{n_x \times n_f}$ are known matrices.

The directed mode is proposed as $(\mathcal{V}, \mathcal{W})$. $\mathcal{V} = \{v_1, v_2, \dots, v_n\}$ represents the set of nodes, and n is the number of nodes. $\mathcal{W} = \{(v_t, v_j), t \neq j\}$ is the set of edges, and g_{tj} is the connectivity. When $g_{tj} = 1$, edges v_t and v_j are connected; when $g_{tj} = 0$, edges v_t and v_j are unconnected. \mathcal{G} is a Laplacian matrix described as $\mathcal{G} = [g_{tj}], t \neq j$. By considering the undirected graph, \mathcal{G} is defined as a symmetric matrix.

If the Kronecker product and the interconnection of each subsystem are considered, then Eq. (1) is

equivalent to

$$\begin{cases} x(k+1) = \mathcal{A}_i x(k) + \mathcal{B}_i u(k) + \mathcal{D}_i \eta(k) + \mathcal{E}_i f(k), \\ y(k) = \mathcal{C}_i x(k), \end{cases} \quad (2)$$

where

$$\begin{aligned} x(k) &= [x_1^T(k), \dots, x_N^T(k)]^T, \quad u(k) = [u_1^T(k), \dots, u_N^T(k)]^T, \\ \eta(k) &= [\eta_1^T(k), \dots, \eta_N^T(k)]^T, \quad f(k) = [f_1^T(k), \dots, f_N^T(k)]^T, \\ \begin{cases} \mathcal{A}_i = I_N \otimes A_{t,\sigma(k)} - a(\mathcal{G} \otimes (\Lambda C_{t,\sigma(k)})) \in \mathbb{R}^{Nn_x \times Nn_x}, \\ \mathcal{B}_i = I_N \otimes B_{t,\sigma(k)} \in \mathbb{R}^{Nn_x \times Nn_u}, \\ \mathcal{D}_i = I_N \otimes D_{t,\sigma(k)} \in \mathbb{R}^{Nn_x \times Nn_\eta}, \\ \mathcal{E}_i = I_N \otimes E_{t,\sigma(k)} \in \mathbb{R}^{Nn_x \times Nn_f}, \\ \mathcal{C}_i = I_N \otimes C_{t,\sigma(k)} \in \mathbb{R}^{Nn_y \times Nn_x}. \end{cases} \end{aligned}$$

Definition 1. For a switching signal $\sigma(k)$ and $0 \leq k_1 \leq k_2$, $N_\sigma(k_1, k_2)$ denotes the number of discontinuities of $\sigma(k)$ in the interval $k \in [k_1, k_2]$. If there exist the chatter bound N_0 and τ , the inequality satisfies $N_\sigma(k_1, k_2) \leq N_0 + \frac{k_2 - k_1}{\tau}$, where $\tau > 0$ denotes the ADT.

Assumption 1.

$$\text{rank} \begin{bmatrix} I_{n_x} & R_{t,\sigma(k)} \\ C_{t,\sigma(k)} & 0_{n_y \times (n_f + n_\eta)} \end{bmatrix} = n_x + n_f + n_\eta,$$

where $R_{t,\sigma(k)} = [D_{t,\sigma(k)} \ E_{t,\sigma(k)}]$.

Assumption 2.

$$\text{rank} \begin{bmatrix} sI_{n_x} - A_{t,\sigma(k)} & R_{t,\sigma(k)} \\ C_{t,\sigma(k)} & 0_{n_y \times (n_f + n_\eta)} \end{bmatrix} = n_x + n_f + n_\eta,$$

where s satisfies $\|s\| \geq 1$.

Remark 1. From a practical perspective, Assumptions 1 and 2 are necessary and sufficient conditions for observer design. Combining the observer matching conditions with the above two assumptions, design methods have been developed in different types of systems with unknown input signals, such as switched descriptor systems, multi-agent systems, and continuous systems [46–50].

Lemma 1.

$$\text{rank}(\mathcal{C}_i \mathcal{R}_i) = \text{rank}(\mathcal{R}_i), \quad \mathcal{R}_i = \begin{bmatrix} \mathcal{D}_i & \mathcal{E}_i \end{bmatrix}.$$

Proof. According to Assumption 1, we can obtain

$$\begin{aligned} \text{rank} \begin{bmatrix} I_{n_x} & R_{t,\sigma(k)} \\ C_{t,\sigma(k)} & 0 \end{bmatrix} &= \text{rank} \left\{ \begin{bmatrix} I_{n_x} & 0 \\ -C_{t,\sigma(k)} & I_{n_y} \end{bmatrix} \times \begin{bmatrix} I_{n_x} & R_{t,\sigma(k)} \\ C_{t,\sigma(k)} & 0 \end{bmatrix} \begin{bmatrix} I_{n_x} & -R_{t,\sigma(k)} \\ 0 & I_{n_f + n_\eta} \end{bmatrix} \right\} \\ &= \text{rank} \begin{bmatrix} I_{n_x} & 0 \\ 0 & -C_{t,\sigma(k)} R_{t,\sigma(k)} \end{bmatrix}. \end{aligned}$$

We obtain $\text{rank}(C_{t,\sigma(k)} R_{t,\sigma(k)}) = n_f + n_\eta$.

$$\begin{aligned} \text{rank}(\mathcal{C}_i \mathcal{R}_i) &= \text{rank} \left(\begin{bmatrix} C_{t,\sigma(k)} R_{t,\sigma(k)} & & \\ & \ddots & \\ & & C_{t,\sigma(k)} R_{t,\sigma(k)} \end{bmatrix} \right) \\ &= N \text{rank}(C_{t,\sigma(k)} R_{t,\sigma(k)}) \\ &= N(n_f + n_\eta) \\ &= \text{rank}(\mathcal{R}_i). \end{aligned}$$

Lemma 2. On the basis of Assumption 2, we obtain

$$\begin{bmatrix} sI_{Nn_x} - \mathcal{A}_i & \mathcal{R}_i \\ \mathcal{C}_i & 0 \end{bmatrix} = N(n_x + n_f + n_\eta),$$

which holds for all s with $\|s\| \geq 1$.

Proof. For implicitness, we only let $N = 2$ and have

$$\begin{aligned} & \text{rank} \begin{bmatrix} sI_{Nn_x} - \mathcal{A}_i & \mathcal{R}_i \\ \mathcal{C}_i & 0 \end{bmatrix} \\ &= \text{rank} \begin{bmatrix} sI_{n_x} - A_{t,\sigma(k)} + ag_{11}(\Lambda C_{t,\sigma(k)}) & ag_{12}(\Lambda C_{t,\sigma(k)}) & R_{t,\sigma(k)} & 0 \\ ag_{21}(\Lambda C_{t,\sigma(k)}) & sI_{n_x} - A_{t,\sigma(k)} + ag_{22}(\Lambda C_{t,\sigma(k)}) & 0 & R_{t,\sigma(k)} \\ C_{t,\sigma(k)} & 0 & 0 & 0 \\ 0 & C_{t,\sigma(k)} & 0 & 0 \end{bmatrix} \\ &= \text{rank} \left\{ \begin{bmatrix} I_{n_x} & 0 & -ag_{11}\Lambda & -ag_{12}\Lambda \\ 0 & I_{n_x} & -ag_{21}\Lambda & -ag_{22}\Lambda \\ 0 & 0 & I_{n_y} & 0 \\ 0 & 0 & 0 & I_{n_y} \end{bmatrix} \times \begin{bmatrix} sI_{n_x} - A_{t,\sigma(k)} + ag_{11}(\Lambda C_{t,\sigma(k)}) & ag_{12}(\Lambda C_{t,\sigma(k)}) & R_{t,\sigma(k)} & 0 \\ ag_{21}(\Lambda C_{t,\sigma(k)}) & sI_{n_x} - A_{t,\sigma(k)} + ag_{22}(\Lambda C_{t,\sigma(k)}) & 0 & R_{t,\sigma(k)} \\ C_{t,\sigma(k)} & 0 & 0 & 0 \\ 0 & C_{t,\sigma(k)} & 0 & 0 \end{bmatrix} \right\} \\ &= \text{rank} \begin{bmatrix} sI_{n_x} - A_{t,\sigma(k)} & 0 & R_{t,\sigma(k)} & 0 \\ 0 & sI_{n_x} - A_{t,\sigma(k)} & 0 & R_{t,\sigma(k)} \\ C_{t,\sigma(k)} & 0 & 0 & 0 \\ 0 & C_{t,\sigma(k)} & 0 & 0 \end{bmatrix} = 2(n_x + n_f + n_\eta). \end{aligned}$$

Remark 2. Note that Lemmas 1 and 2 are used to guarantee the asymptotic convergence of error systems. It is proven that the preconditions satisfied for the subsystems are guaranteed for the overall system.

To facilitate the observer design, the following conditions should be considered.

- (1) When $f(k) = 0$ and $\eta(k) = 0$, the stability of the error system is guaranteed.
- (2) The residual $r(k)$ is robust against the disturbance $\eta(k)$, and the following mixed $L_2 - L_\infty/H_\infty$ performance holds:

$$\sum_{k=0}^{\infty} \{(1 - b)r^T(k)r(k) - \mu^2\eta^T(k)\eta(k)\} + br^T(k)r(k) < 0. \tag{3}$$

If $b = 0$ is selected, the H_∞ performance holds; if $b = 1$ is selected, the $L_2 - L_\infty$ performance holds.

- (3) The generated residual $r(k)$ is sensitive to the fault $f(k)$, and the following H_- performance holds:

$$\|r(k)\|^2 > \beta^2\|f(k)\|^2, \tag{4}$$

where $|\omega| \leq \omega_l$, and ω_l is the low-frequency domain.

Remark 3. Inequality (3) is clearly a unified framework. If parameter $b = 0$ is selected, it can be turned into the H_∞ performance; if parameter $b = 1$ is selected, the $L_2 - L_\infty$ performance holds. Therefore, condition (3) is more general than the condition that considers a single control problem.

3 Fault detection scheme

In this section, an observer using the mixed $L_2 - L_\infty/H_\infty$ index and the H_- index is proposed to generate residuals. The subsystems' stability is considered, and LMI conditions are derived because of the Lyapunov function and the ADT method.

3.1 Observer design

The observer is defined as

$$\begin{cases} z(k+1) = F_i z(k) + T_i \mathcal{B}_i u(k) + L_i y(k), \\ \hat{x}(k) = z(k) + H_i y(k), \\ \hat{y}(k) = \mathcal{C}_i \hat{x}(k), \end{cases} \quad (5)$$

where F_i , T_i , L_i , and H_i are matrices that will be determined, and $\hat{x}(k)$ is the estimation of state $x(k)$. Based on Assumption 1, for matrices T_i and H_i , the following equation is satisfied:

$$\begin{bmatrix} T_i & H_i \end{bmatrix} \begin{bmatrix} I_{Nn_x} \\ \mathcal{C}_i \end{bmatrix} = I_{Nn_x}. \quad (6)$$

Let $M_i = \begin{bmatrix} I_{Nn_x} \\ \mathcal{C}_i \end{bmatrix} \in \mathbb{R}^{(Nn_x+Nn_y) \times Nn_x}$. Note that $M_i^T M_i$ is nonsingular, $M_i^+ = (M_i^T M_i)^{-1} M_i^T$. Z_i is an arbitrary matrix, and the general solution to (6) is provided as

$$\begin{bmatrix} T_i & H_i \end{bmatrix} = M_i^+ - Z_i (I_{Nn_x+Nn_y} - M_i M_i^+), \quad (7)$$

where

$$\begin{aligned} T_i &= (M_i^+ - Z_i (I_{Nn_x+Nn_y} - M_i M_i^+)) \begin{bmatrix} I_{Nn_x} \\ \mathbf{0}_{Nn_y \times Nn_x} \end{bmatrix}, \\ H_i &= (M_i^+ - Z_i (I_{Nn_x+Nn_y} - M_i M_i^+)) \begin{bmatrix} \mathbf{0}_{Nn_x \times Nn_y} \\ I_{Nn_y} \end{bmatrix}. \end{aligned}$$

Let $e(k) = x(k) - \hat{x}(k) = T_i x(k) - z(k)$ and $r(k) = y(k) - \hat{y}(k) = \mathcal{C}_i e(k)$ denote the estimation error and the residual signal, respectively. The error dynamic is proposed as

$$\begin{aligned} e(k+1) &= T_i x(k+1) - z(k+1) \\ &= T_i (\mathcal{A}_i x(k) + \mathcal{B}_i u(k) + \mathcal{D}_i \eta(k) + \mathcal{E}_i f(k)) \\ &\quad - (F_i (\hat{x}(k) - H_i y(k)) + T_i \mathcal{B}_i u(k) + L_i y(k)) \\ &= F_i e(k) + (T_i \mathcal{A}_i - F_i + (F_i H_i - L_i) \mathcal{C}_i) x(k) + T_i \mathcal{D}_i \eta(k) + T_i \mathcal{E}_i f(k). \end{aligned} \quad (8)$$

If $T_i \mathcal{A}_i - F_i + (F_i H_i - L_i) \mathcal{C}_i = 0$ holds and the following equations can be derived as

$$F_i = T_i \mathcal{A}_i + (F_i H_i - L_i) \mathcal{C}_i, \quad L_i = F_i H_i - J_i, \quad (9)$$

then according to (8) and (9), the error dynamic is written as

$$\begin{cases} e(k+1) = F_i e(k) + T_i \mathcal{D}_i \eta(k) + T_i \mathcal{E}_i f(k), \\ r(k) = \mathcal{C}_i e(k). \end{cases} \quad (10)$$

3.2 Stability analysis and disturbance robustness

The sufficient conditions for stability and disturbance robustness are given in Theorem 1. Assuming that $\eta(k) = 0$ and $f(k) = 0$ are satisfied, the first part is the stability analysis. Letting $f(k) = 0$, the second part is provided to establish the mixed $L_2 - L_\infty/H_\infty$ performance, and the performance index can be calculated.

Theorem 1. Given any $i \neq j$, $0 < \lambda_1 < 1$, $\lambda_2 > 1$, there are matrices G_i , symmetric positive definite matrices $P_{\eta i} = P_{\eta i}^T > 0$, $P_{\eta j} = P_{\eta j}^T > 0$, and scalars a_1 , a_2 such that the following conditions hold:

$$\tau > \tau^* = -\frac{\ln \lambda_2}{\ln \lambda_1}, \quad P_{\eta i} < \lambda_2 P_{\eta j}, \quad (11)$$

$$\begin{bmatrix} -\lambda_1 P_{\eta i} + a_1 \text{He}\{G_i T_i \mathcal{A}_i + W_i \mathcal{C}_i\} - a_1 G_i + \mathcal{A}_i^T T_i^T G_i^T + \mathcal{C}_i^T W_i^T \\ * \\ P_{\eta i} - G_i - G_i^T \end{bmatrix} < 0, \quad (12)$$

$$\begin{bmatrix} \Xi_{11} & \Xi_{12} & \Xi_{13} \\ * & \Xi_{22} & \Xi_{23} \\ * & * & \Xi_{33} \end{bmatrix} < 0, \tag{13}$$

$$\begin{bmatrix} -P_{\eta_i} & C_i^T \\ C_i & -\frac{1}{b}I \end{bmatrix} < 0, \tag{14}$$

$$\begin{cases} \Xi_{11} = -P_{\eta_i} + (1-b)C_i^T C_i + \text{He}\{a_2(G_i T_i A_i + W_i C_i)\}, \\ \Xi_{12} = a_2 G_i T_i D_i, \\ \Xi_{13} = -a_2 G_i + A_i^T T_i^T G_i^T + C_i^T W_i^T, \\ \Xi_{22} = -\mu^2 I, \\ \Xi_{23} = D_i^T T_i^T G_i^T, \\ \Xi_{33} = P_{\eta_i} - G_i - G_i^T. \end{cases}$$

Proof. (1) Assuming that $f(k) = 0$ and $\eta(k) = 0$, the Lyapunov function is chosen as

$$V_{1i}(k) = e^T(k) P_{\eta_i} e(k). \tag{15}$$

The difference of (15) is taken as

$$\Delta V_{1i}(k) = V_{1i}(k+1) - V_{1i}(k) = e^T(k) ((F_i)^T P_{\eta_i} F_i - P_{\eta_i}) e(k). \tag{16}$$

Assume that $\Delta V_{1i}(k) < 0$ makes the stability condition hold. Then, $0 < \lambda_1 < 1$, $\Delta V_{1i}(k) < 0$ is proposed as

$$\begin{aligned} \Delta W_{1i}(k) &= V_{1i}(k+1) - \lambda_1 V_{1i}(k) \\ &= e^T(k) ((F_i)^T P_{\eta_i} F_i - \lambda_1 P_{\eta_i}) e(k) \\ &= e^T(k) \mathcal{H}_{1i} e(k) < 0, \end{aligned} \tag{17}$$

which is equivalent to the following inequality:

$$(F_i)^T P_{\eta_i} F_i - \lambda_1 P_{\eta_i} < 0. \tag{18}$$

Let $M_{1i} = a_1 G_i$. A sufficient condition of (18) is proposed as

$$\begin{bmatrix} -\lambda_1 P_{\eta_i} + M_{1i} F_i + (F_i)^T M_{1i}^T - M_{1i} + (F_i)^T G_i^T \\ * & P_{\eta_i} - G_i - G_i^T \end{bmatrix} < 0. \tag{19}$$

On the basis of $F_i = T_i A_i + J_i C_i$ and $W_i = G_i J_i$, Eq. (19) is rewritten as (13), and we obtain

$$\Delta V_{1i}(k) = e^T(k) ((F_i)^T P_{\eta_i} F_i - P_{\eta_i}) e(k) < (\lambda_1 - 1) V_{1i}(k), \tag{20}$$

i.e., $V_{1i}(k+1) < \lambda_1 V_{1i}(k)$. Suppose the condition $V_{1i}(k) < \lambda_1^{k-k_s} V_{1i}(k_s)$ holds for the interval $[k_s, k)$.

Considering that $P_{\eta_i} < \lambda_2 P_{\eta_j}$ and $\sigma(k_{s-1}) = j$, we have

$$V_{1i}(k_s) < \lambda_2 V_{1\sigma(k_{s-1})}(k_{s-1}). \tag{21}$$

After combining (20) with (21), we obtain

$$\begin{aligned} V_{1i}(k) &< \lambda_1^{k-k_s} V_{1i}(k_s) \\ &< \lambda_1^{k-k_{s-1}} \lambda_2 V_{1\sigma(k_{s-1})}(k_{s-1}) \\ &< \lambda_1^{k-k_{s-1}} \lambda_2^2 V_{1\sigma(k_{s-2})}(k_{s-1}) \\ &< \lambda_1^{k-k_{s-2}} \lambda_2^2 V_{1\sigma(k_{s-2})}(k_{s-2}) \\ &< \dots < \lambda_1^k \lambda_2^{N_{\sigma(0,k)}} V_{1\sigma(0)}(0) \end{aligned}$$

$$< \lambda_2^{k(\frac{1}{\tau} + \frac{\ln \lambda_2}{\ln \lambda_1})} V_{1\sigma(0)}(0). \tag{22}$$

It is clear to establish the condition that

$$\gamma_1 e^T(k)e(k) \leq V_{1i}(k) \leq \gamma_2 e^T(k)e(k), \tag{23}$$

where $\gamma_1 = \min \lambda_{\min}(P_{\eta i})$ and $\gamma_2 = \max \lambda_{\max}(P_{\eta i})$. We can obtain $e^T(k)e(k) \leq \frac{\gamma_2}{\gamma_1} \lambda_1^k \lambda_2^{\frac{k}{\tau}} e^T(0)e(0)$. It is proposed as

$$\|e(k)\|^2 \leq \frac{\gamma_2}{\gamma_1} \lambda_1^k \lambda_2^{\frac{k}{\tau}} \|e(0)\|^2 \leq \frac{\gamma_2}{\gamma_1} (\lambda_2)^{k(\frac{1}{\tau} + \frac{\ln \lambda_2}{\ln \lambda_1})} \|e(0)\|^2. \tag{24}$$

On the basis of the above inequality, $\lim_{k \rightarrow \infty} \|e(k)\| = 0$ is satisfied. Assuming that $f(k) = 0$ and $\eta(k) = 0$, the stability of the error system is clearly guaranteed.

(2) When $\eta(k) \neq 0$ and $f(k) = 0$, Eq. (10) is rewritten as

$$\begin{cases} e(k+1) = F_i e(k) + T_i \mathcal{D}_i \eta(k), \\ r(k) = C_i e(k). \end{cases} \tag{25}$$

Let the Lyapunov function

$$V_{2i}(k) = e^T(k)P_{\eta i}e(k). \tag{26}$$

On the basis of (26), the difference can be taken as

$$\begin{aligned} \Delta V_{2i}(k) &= V_{2i}(k+1) - V_{2i}(k) \\ &= e^T(k)(F_i)^T P_{\eta i}(F_i)e(k) + e^T(k)(F_i)^T P_{\eta i}T_i \mathcal{D}_i \eta(k) - e^T(k)P_{\eta i}e(k) \\ &\quad + \eta^T(k)\mathcal{D}_i^T T_i^T P_{\eta i}(F_i)e(k) + \eta^T(k)\mathcal{D}_i^T T_i^T P_{\eta i}T_i \mathcal{D}_i \eta(k). \end{aligned} \tag{27}$$

Define $\mathcal{J}_{1i}(k)$ as

$$\begin{aligned} \mathcal{J}_{1i}(k) &= \Delta V_{2i}(k) + (1-b)r^T(k)r(k) - \mu^2 \eta^T(k)\eta(k) \\ &= \begin{bmatrix} e(k) \\ \eta(k) \end{bmatrix}^T \mathcal{H}_{2i} \begin{bmatrix} e(k) \\ \eta(k) \end{bmatrix} < 0, \end{aligned} \tag{28}$$

which is equivalent to

$$\mathcal{H}_{2i} = \begin{bmatrix} (F_i)^T P_{\eta i}(F_i) - P_{\eta i} + (1-b)C_i^T C_i & * \\ \mathcal{D}_i^T T_i^T P_{\eta i} F_i & \mathcal{D}_i^T T_i^T P_{\eta i} T_i \mathcal{D}_i - \mu^2 I \end{bmatrix} < 0. \tag{29}$$

On the basis of (29) and Finsler's Lemma [51], it follows that

$$\Psi_{1i} + \Phi_{1i}^T P_{\eta i} \Phi_{1i} < 0, \tag{30}$$

where $\Psi_{1i} = \begin{bmatrix} -P_{\eta i} + (1-b)C_i^T C_i & 0 \\ 0 & -\mu^2 I \end{bmatrix}$, $\Phi_{1i} = [F_i \ T_i \mathcal{D}_i]$, and $M_{2i} = \begin{bmatrix} a_2 G_i \\ 0 \end{bmatrix}$.

A sufficient condition of (30) is provided as

$$\begin{bmatrix} \Psi_{1i} + M_{2i}\Phi_{1i} + \Phi_{1i}^T M_{2i}^T - M_{2i} + \Phi_{1i}^T G_i^T \\ * & P_{\eta i} - G_i - G_i^T \end{bmatrix} < 0. \tag{31}$$

Substituting Ψ_{1i} , Φ_{1i} , and M_{2i} into (31), this condition is deduced as

$$\begin{bmatrix} \hat{\Xi}_{11} & \hat{\Xi}_{12} & \hat{\Xi}_{13} \\ * & \hat{\Xi}_{22} & \hat{\Xi}_{23} \\ * & * & \hat{\Xi}_{33} \end{bmatrix} < 0, \tag{32}$$

where

$$\begin{cases} \hat{\Xi}_{11} = -P_{\eta i} + (1 - b)\mathcal{C}_i^T \mathcal{C}_i + \text{He}\{a_2 G_i F_i\}, \\ \hat{\Xi}_{12} = a_2 G_i T_i \mathcal{D}_i, \\ \hat{\Xi}_{13} = -a_2 G_i + (F_i)^T G_i^T, \\ \hat{\Xi}_{22} = -\mu^2 I, \\ \hat{\Xi}_{23} = \mathcal{D}_i^T T_i^T G_i^T, \\ \hat{\Xi}_{33} = P_{\eta i} - G_i - G_i^T. \end{cases}$$

On the basis of $F_i = T_i \mathcal{A}_i + J_i \mathcal{C}_i$ and $W_i = G_i J_i$, Eq. (32) is rewritten as (13). Note that $\mathcal{J}_{1i}(k) < 0$ is satisfied, and the following inequality holds:

$$\sum_{k=0}^{\infty} \{(1 - b)r^T(k)r(k) - \mu^2 \eta^T(k)\eta(k)\} < -V_{2i}(k). \quad (33)$$

Because of (14), we obtain

$$\begin{aligned} br^T(k)r(k) - V_{2i}(k) &= be^T(k)\mathcal{C}_i^T \mathcal{C}_i e(k) - e^T(k)P_{\eta i} e(k) \\ &= e^T(k)(b\mathcal{C}_i^T \mathcal{C}_i - P_{\eta i})e(k) < 0. \end{aligned} \quad (34)$$

According to (33) and (34), the following inequality can be established:

$$\sum_{k=0}^{\infty} \{(1 - b)r^T(k)r(k) - \mu^2 \eta^T(k)\eta(k)\} + br^T(k)r(k) < 0. \quad (35)$$

3.3 Fault sensitivity

Note that the sufficient conditions of H_- fault sensitivity when fault signals are considered to belong to a finite-frequency domain are given in Theorem 2.

Theorem 2. Given any $i \neq j$, $0 < \lambda_1 < 1$, and $\lambda_2 > 1$, there are matrices K and G_i , symmetric positive definite matrices $P_{fi} = P_{fi}^T > 0$, $P_{fj} = P_{fj}^T > 0$, $Q_{fi} = Q_{fi}^T > 0$, and scalars a_3, a_4 such that the following conditions hold:

$$P_{fi} < \lambda_2 P_{fj}, \quad (36)$$

$$\begin{bmatrix} -\lambda_1 P_{fi} + a_3 \text{He}\{G_i T_i \mathcal{A}_i + W_i \mathcal{C}_i\} - a_3 G_i + \mathcal{A}_i^T T_i^T G_i^T + \mathcal{C}_i^T W_i^T \\ * & P_{fi} - G_i - G_i^T \end{bmatrix} < 0, \quad (37)$$

$$\begin{bmatrix} \Sigma_{11} & \Sigma_{12} & \Sigma_{13} \\ * & \Sigma_{22} & \Sigma_{23} \\ * & * & \Sigma_{33} \end{bmatrix} < 0, \quad (38)$$

$$\begin{cases} \Sigma_{11} = -\lambda_1 P_{fi} - 2 \cos(\omega_l) Q_{fi} - \mathcal{C}_i^T \mathcal{C}_i + \text{He}\{a_4 (G_i T_i \mathcal{A}_i + W_i \mathcal{C}_i)\}, \\ \Sigma_{12} = (\mathcal{A}_i^T T_i^T G_i^T + \mathcal{C}_i^T W_i^T) K + a_4 G_i T_i \mathcal{E}_i, \\ \Sigma_{13} = -a_4 G_i + Q_{fi} + \mathcal{A}_i^T T_i^T G_i^T + \mathcal{C}_i^T W_i^T, \\ \Sigma_{22} = \beta^2 I + \text{He}\{K^T G_i T_i \mathcal{E}_i\}, \\ \Sigma_{23} = \mathcal{E}_i^T T_i^T G_i^T - K^T G_i, \\ \Sigma_{33} = P_{fi} - G_i - G_i^T. \end{cases}$$

Proof. When $\eta(k) = 0$, system (10) is proposed as

$$\begin{cases} e(k + 1) = F_i e(k) + T_i \mathcal{E}_i f(k), \\ r(k) = \mathcal{C}_i e(k). \end{cases} \quad (39)$$

The Lyapunov function is given as

$$V_{3i}(k) = e^T(k)P_{fi}e(k). \quad (40)$$

Based on the above function, the difference can be taken as

$$\begin{aligned} \Delta V_{3i}(k) &= V_{3i}(k+1) - V_{3i}(k) \\ &= (F_i e(k) + T_i \mathcal{E}_i f(k))^T P_{fi} (F_i e(k) + T_i \mathcal{E}_i f(k)) - e^T(k) P_{fi} e(k). \end{aligned} \quad (41)$$

According to inequality (37), $V_{3i}(k+1) < \lambda_1 V_{3i}(k)$ is satisfied. Thus, $V_{3i}(k) < \lambda_1^{k-k_s} V_{3i}(k_s)$. Considering that $P_{fi} < \lambda_2 P_{fj}$ and $\sigma(k_{s-1}) = j$, we have

$$V_{3i}(k_s) < \lambda_2 V_{3\sigma(k_{s-1})}(k_{s-1}). \quad (42)$$

By combining $V_{3i}(k+1) < \lambda_1 V_{3i}(k)$ with (42), this function can be obtained as

$$\begin{aligned} V_{3i}(k) &< \lambda_1^{k-k_s} V_{3i}(k_s) \\ &< \lambda_1^{k-k_{s-1}} \lambda_2 V_{3\sigma(k_{s-1})}(k_{s-1}) \\ &< \lambda_1^{k-k_{s-1}} \lambda_2^2 V_{3\sigma(k_{s-2})}(k_{s-1}) \\ &< \lambda_1^{k-k_{s-2}} \lambda_2^2 V_{3\sigma(k_{s-2})}(k_{s-2}) \\ &< \dots < \lambda_1^k \lambda_2^{N_{\sigma(0,k)}} V_{3\sigma(0)}(0) \\ &< \lambda_2^{k(\frac{1}{\tau} + \frac{\ln \lambda_2}{\ln \lambda_1})} V_{3\sigma(0)}(0). \end{aligned} \quad (43)$$

Note that

$$\gamma_3 e^T(k) e(k) \leq V_{3i}(k) \leq \gamma_4 e^T(k) e(k), \quad (44)$$

where $\gamma_3 = \min \lambda_{\min}(P_{fi})$, $\gamma_4 = \max \lambda_{\max}(P_{fi})$.

According to (43), $e^T(k) e(k) \leq \frac{\gamma_4}{\gamma_3} \lambda_1^k \lambda_2^{\frac{k}{\tau}} e^T(0) e(0)$ is obtained, which can be described as

$$\|e(k)\|^2 \leq \frac{\gamma_4}{\gamma_3} \lambda_1^k \lambda_2^{\frac{k}{\tau}} \|e(0)\|^2 \leq \frac{\gamma_4}{\gamma_3} (\lambda_2)^{k(\frac{1}{\tau} + \frac{\ln \lambda_4}{\ln \lambda_3})} \|e(0)\|^2. \quad (45)$$

On the basis of the above inequality, $\lim_{k \rightarrow \infty} \|e(k)\| = 0$ is satisfied. Assuming that $f(k)$ belongs to a low-frequency domain, i.e., $|\omega| \leq \omega_l$, the following inequality is clearly satisfied:

$$\sum_{k=0}^{\infty} ((e(k+1) - e(k))(e(k+1) - e(k))^T) < \left(2 \sin\left(\frac{\omega_l}{2}\right)\right)^2 \sum_{k=0}^{\infty} e(k) e^T(k). \quad (46)$$

Inequality (46) is proposed as

$$\sum_{k=0}^{\infty} ((e(k+1) - e(k))(e(k+1) - e(k))^T) < (2 - 2 \cos(\omega_l)) \sum_{k=0}^{\infty} e(k) e^T(k). \quad (47)$$

According to inequality (45) and $\lim_{k \rightarrow \infty} \|e(k)\| = 0$, the following condition holds:

$$\sum_{k=0}^{\infty} e(k+1) e^T(k+1) = \sum_{k=0}^{\infty} e(k) e^T(k).$$

Assuming that the zero initial condition holds, Eq. (47) is equivalent to $\sum_{k=0}^{\infty} S < 0$, where $S = -e(k+1) e^T(k) - e(k) e^T(k+1) + 2 \cos(\omega_l) e(k) e^T(k)$. Let $\Delta \mathcal{W}_{2i}(k) = V_{3i}(k+1) - \lambda_1 V_{3i}(k)$ and

$$\begin{aligned} \text{tr}(Q_{fi} S) &= \text{tr}[Q_{fi} (-e(k+1) e^T(k) - e(k) e^T(k+1) + 2 \cos(\omega_l) e(k) e^T(k))] \\ &= -e^T(k+1) Q_{fi} e(k) - e^T(k) Q_{fi} e(k+1) + 2 \cos(\omega_l) e^T(k) Q_{fi} e(k). \end{aligned} \quad (48)$$

According to (48), $\mathcal{J}_{2i}(k)$ can be defined as

$$\begin{aligned} \mathcal{J}_{2i}(k) &= \Delta \mathcal{W}_{2i}(k) + \beta^2 f^T(k) f(k) - r^T(k) r(k) - \text{tr}(Q_{fi} S) \\ &= (F_i e(k) + T_i \mathcal{E}_i f(k))^T P_{fi} (F_i e(k) + T_i \mathcal{E}_i f(k)) - \lambda_1 e^T(k) P_{fi} e(k) \\ &\quad + \beta^2 f^T(k) f(k) - e^T(k) \mathcal{C}_i^T \mathcal{C}_i e(k) + (F_i e(k) + T_i \mathcal{E}_i f(k))^T Q_{fi} e(k) \\ &\quad + e^T(k) Q_{fi} (F_i e(k) + T_i \mathcal{E}_i f(k)) - 2 \cos(\omega_l) e^T(k) Q_{fi} e(k) \\ &= \begin{bmatrix} e(k) \\ f(k) \end{bmatrix}^T \mathcal{H}_{3i} \begin{bmatrix} e(k) \\ f(k) \end{bmatrix}. \end{aligned}$$

Assume that $\mathcal{J}_{2i}(k) < 0$, meaning that $\mathcal{H}_{3i} < 0$. Equivalently,

$$\Psi_{2i} + \Phi_{2i}^T \bar{Q}_i^T + \bar{Q}_i \Phi_{2i} + \Phi_{2i}^T P_{fi} \Phi_{2i} < 0, \tag{49}$$

where $\Psi_{2i} = \begin{bmatrix} -\lambda_1 P_{fi} - 2 \cos(\omega_l) Q_{fi} - C_i^T C_i & 0 \\ * & \beta^2 I \end{bmatrix}$, $\Phi_{2i} = [F_i \ T_i \mathcal{E}_i]$, and $\bar{Q}_i = \begin{bmatrix} Q_{fi} \\ 0 \end{bmatrix}$.

The sufficient condition of (49) is provided as

$$\begin{bmatrix} \Psi_{2i} + M_{3i} \Phi_{2i} + \Phi_{2i}^T M_{3i}^T - M_{3i} + \bar{Q}_i + \Phi_{2i}^T G_i^T \\ * & P_{fi} - G_i - G_i^T \end{bmatrix} < 0. \tag{50}$$

Substituting Ψ_{2i} , Φ_{2i} , \bar{Q}_i , and $M_{3i} = \begin{bmatrix} a_4 G_i \\ K^T G_i \end{bmatrix}$ into (50), the following inequality holds:

$$\begin{bmatrix} \hat{\Sigma}_{11} & \hat{\Sigma}_{12} & \hat{\Sigma}_{13} \\ * & \hat{\Sigma}_{22} & \hat{\Sigma}_{23} \\ * & * & \hat{\Sigma}_{33} \end{bmatrix} < 0, \tag{51}$$

where

$$\begin{cases} \hat{\Sigma}_{11} = -\lambda_1 P_{fi} - 2 \cos(\omega_l) Q_{fi} - C_i^T C_i + a_4 \text{He}\{G_i F_i\}, \\ \hat{\Sigma}_{12} = (F_i)^T G_i^T K + a_4 G_i T_i \mathcal{E}_i + (F_i)^T T_i \mathcal{E}_i, \\ \hat{\Sigma}_{13} = -a_4 G_i + Q_{fi} + (F_i)^T G_i^T, \\ \hat{\Sigma}_{22} = \beta^2 I + \text{He}\{K^T G_i T_i \mathcal{E}_i\} + (T_i \mathcal{E}_i)^T T_i \mathcal{E}_i, \\ \hat{\Sigma}_{23} = (T_i \mathcal{E}_i)^T G_i^T - K^T G_i, \\ \hat{\Sigma}_{33} = P_{fi} - G_i - G_i^T. \end{cases}$$

On the basis of (51), we obtain

$$\mathcal{J}_{2i}(k) = \Delta \mathcal{W}_{2i}(k) + \beta^2 f^T(k) f(k) - r^T(k) r(k) - \text{tr}(Q_{fi} S) < 0.$$

It can be deduced that

$$\Delta V_{3i}(k) + \beta^2 f^T(k) f(k) - r^T(k) r(k) - \text{tr}(Q_{fi} S) < 0. \tag{52}$$

Note that

$$\begin{aligned} & \sum_{k=0}^{\infty} \{ \Delta V_{3i}(k) + \beta^2 f^T(k) f(k) - r^T(k) r(k) - \text{tr}(Q_{fi} S) \} \\ & = V_{3i}(\infty) - V_{3i}(0) + \beta^2 \sum_{k=0}^{\infty} f^T(k) f(k) - \sum_{k=0}^{\infty} r^T(k) r(k) - \sum_{k=0}^{\infty} \text{tr}(Q_{fi} S). \end{aligned} \tag{53}$$

The zero initial condition clearly holds. Obviously, $V_{3i}(0) = 0$. Based on (45), $\lim_{k \rightarrow \infty} \|e(k)\| = 0$ and $V_{3i}(\infty) = 0$ are satisfied. On the basis of $\sum_{k=0}^{\infty} S < 0$ and $Q_{fi} > 0$, we obtain

$$\sum_{k=0}^{\infty} \text{tr}(Q_{fi} S) = \text{tr} \left(\sum_{k=0}^{\infty} (Q_{fi} S) \right) < 0. \tag{54}$$

According to (53) and (54), it can be deduced that $\mathcal{J}_{3i}(k) < 0$, meaning that $\beta^2 \sum_{k=0}^{\infty} f^T(k) f(k) < \sum_{k=0}^{\infty} r^T(k) r(k)$.

3.4 Detection strategy

In this subsection, the following theorem is proposed to make the proposed method hold. We calculate matrices to complete the observer design such that conditions (3) and (4) are satisfied.

Theorem 3. Given any $i \neq j$, $0 < \lambda_1 < 1$, and $\lambda_2 > 1$, there are matrices G_i , K , symmetric positive definite matrices $P_{\eta i} = P_{\eta j}^T > 0$, $P_{\eta j} = P_{\eta i}^T > 0$, $P_{fi} = P_{fi}^T > 0$, $P_{fj} = P_{fj}^T > 0$, $Q_{fi} = Q_{fi}^T > 0$, and scalars a_1, a_2, a_3, a_4 such that inequalities (11)–(14), (36)–(38) hold.

Proof. Similar to Theorems 1 and 2, the process of proof is performed by setting $F_i = T_i \mathcal{A}_i + J_i \mathcal{C}_i$ and $W_i = G_i J_i$, which is omitted here.

In solving the following optimization problem, performance indexes μ and β are obtained:

$$\begin{aligned} & \min \mu + \beta, \\ & \text{s.t. Eqs. (11)–(14), (36)–(38).} \end{aligned}$$

After W_i and G_i are obtained, matrices J_i , F_i , and L_i are calculated using the following equalities:

$$J_i = G_i^{-1} W_i, \quad F_i = T_i \mathcal{A}_i + J_i \mathcal{C}_i, \quad L_i = F_i H_i - J_i.$$

Remark 4. Based on Theorem 3, the conditions of the proposed method, which guarantee the system's stability and performance analysis as LMIs, are proposed by introducing parameters a_1, a_2, a_3, a_4, G_i , and K , which need to be designed beforehand under the ADT method.

As shown in the above discussion, the switched system is affected by the fault in the finite-frequency domain and the disturbance with a known bound. To assess whether the fault occurs, the residual evaluation function is determined as $J_r = \|r(k)\|$. Moreover, the corresponding threshold J_{th} is chosen as $J_{th} = \sup_{f(k)=0} J_r$ when the system has no fault.

When the residual exceeds the threshold, the fault detection is clearly achieved. The detection scheme gives the alarm rule by adopting the following detection logic, which compares the evaluation function with the corresponding threshold:

$$\begin{cases} J_r \leq J_{th} \Rightarrow \text{the system with no alarm,} \\ J_r > J_{th} \Rightarrow \text{the system with alarm.} \end{cases}$$

4 Fault isolation scheme

4.1 Observer design

System (2) is rewritten as

$$\begin{cases} x(k+1) = \mathcal{A}_i x(k) + \mathcal{B}_i u(k) + \mathcal{D}_i \eta(k) + \bar{\mathcal{E}}_{it} \bar{f}_t(k) + \mathcal{E}_{it} f_t(k), \\ y(k) = \mathcal{C}_i x(k), \end{cases} \quad (55)$$

where $f_t(k)$ is the t -th ($t = 1, \dots, N$) row vector of $f(k)$, and \mathcal{E}_{it} is the t -th column component of \mathcal{E}_i . $\bar{f}_t(k)$ is a column vector that is derived after removing $f_t(k)$, and $\bar{\mathcal{E}}_{it}$ is the matrix obtained by removing the t -th column of \mathcal{E}_i . The notations are provided as

$$\bar{f}_t(k) = \left[f_1^T(k) \cdots f_{t-1}^T(k) \quad f_{t+1}^T(k) \cdots f_N^T(k) \right]^T \in \mathbb{R}^{(N-1)n_f},$$

$$\mathcal{E}_i = \left[\mathcal{E}_{i1} \cdots \mathcal{E}_{iN} \right] \in \mathbb{R}^{Nn_x \times Nn_f},$$

$$\bar{\mathcal{E}}_{it} = \left[\mathcal{E}_{i1} \cdots \mathcal{E}_{i(t-1)} \quad \mathcal{E}_{i(t+1)} \cdots \mathcal{E}_{iN} \right] \in \mathbb{R}^{Nn_x \times (N-1)n_f}.$$

Let $\bar{x}(k) = [x(k) \quad \bar{f}_t(k)]$, and system (55) is rewritten as

$$\begin{cases} \bar{N}_t \bar{x}(k+1) = \bar{\mathcal{A}}_{it} \bar{x}(k) + \mathcal{B}_i u(k) + \mathcal{D}_i \eta(k) + \mathcal{E}_{it} f_t(k), \\ \bar{y}(k) = \bar{\mathcal{C}}_{it} \bar{x}(k), \end{cases} \quad (56)$$

where

$$\bar{\mathcal{A}}_{it} = \left[\mathcal{A}_i \quad \bar{\mathcal{E}}_{it} \right], \quad \bar{\mathcal{C}}_{it} = \left[\mathcal{C}_i \quad 0_{Nn_y \times (N-1)n_f} \right],$$

$$\bar{N}_t = \left[I_{Nn_x} \quad 0_{Nn_x \times (N-1)n_f} \right].$$

On the basis of Assumption 1, given matrices \bar{T}_{it} and \bar{H}_{it} , the following equation holds:

$$\begin{bmatrix} \bar{T}_{it} & \bar{H}_{it} \end{bmatrix} \begin{bmatrix} \bar{N}_t \\ \bar{C}_{it} \end{bmatrix} = I_{Nn_x+(N-1)n_f}. \quad (57)$$

The general solution to (57) is provided as

$$\begin{bmatrix} \bar{T}_{it} & \bar{H}_{it} \end{bmatrix} = \bar{M}_{it}^+ - \bar{Z}_{it}(I_{Nn_x+(N-1)n_f} - \bar{M}_{it}\bar{M}_{it}^+), \quad (58)$$

where

$$\begin{aligned} \bar{M}_{it} &= \begin{bmatrix} \bar{N}_t \\ \bar{C}_{it} \end{bmatrix}, \quad \bar{M}_{it}^+ = (\bar{M}_{it}^T \bar{M}_{it})^{-1} \bar{M}_{it}^T, \\ \bar{T}_{it} &= (\bar{M}_{it}^+ - \bar{Z}_{it}(I_{Nn_x+(N-1)n_f} - \bar{M}_{it}\bar{M}_{it}^+)) \begin{bmatrix} I_{Nn_x} \\ \mathbf{0}_{Nn_y \times Nn_x} \end{bmatrix}, \\ \bar{H}_{it} &= (\bar{M}_{it}^+ - \bar{Z}_{it}(I_{Nn_x+(N-1)n_f} - \bar{M}_{it}\bar{M}_{it}^+)) \begin{bmatrix} \mathbf{0}_{Nn_x \times Nn_y} \\ I_{Nn_y} \end{bmatrix}. \end{aligned}$$

By defining $\bar{x}(k) = \bar{z}(k) + \bar{H}_{it}\bar{y}(k)$, Eq. (56) was rewritten as

$$\begin{cases} \bar{z}(k+1) = \bar{T}_{it}\bar{A}_{it}\bar{z}(k) + \bar{T}_{it}\bar{B}_i u(k) + \bar{T}_{it}\bar{D}_i \eta(k) + \bar{T}_{it}\bar{E}_{it} f_t(k) + \bar{T}_{it}\bar{A}_{it}\bar{H}_{it}\bar{y}(k), \\ \bar{y}_z(k) = \bar{C}_{it}\bar{z}(k). \end{cases} \quad (59)$$

According to (59), the t -th observer is designed as

$$\begin{cases} \hat{\bar{z}}_t(k+1) = \bar{T}_{it}\bar{A}_{it}\hat{\bar{z}}_t(k) + \bar{T}_{it}\bar{B}_i u(k) + \bar{T}_{it}\bar{A}_{it}\bar{H}_{it}\bar{y}(k) - \bar{L}_{it}(\bar{y}_z(k) - \bar{C}_{it}\hat{\bar{z}}_t(k)), \\ \hat{\bar{y}}_z(k) = \bar{C}_{it}\hat{\bar{z}}_t(k), \end{cases} \quad (60)$$

where \bar{L}_{it} is the gain matrix.

Let $\bar{e}_{zt}(k) = \bar{z}(k) - \hat{\bar{z}}_t(k)$ and $\bar{r}(k) = \bar{y}_z(k) - \hat{\bar{y}}_z(k) = \bar{C}_{it}\bar{e}_{zt}(k)$ denote the state estimate error and the residual signal, respectively. Then, the error dynamic is derived as

$$\begin{aligned} \bar{e}_{zt}(k+1) &= \bar{z}(k+1) - \hat{\bar{z}}_t(k+1) \\ &= (\bar{T}_{it}\bar{A}_{it} + \bar{L}_{it}\bar{C}_{it})\bar{e}_{zt}(k) + \bar{T}_{it}\bar{D}_i \eta(k) + \bar{T}_{it}\bar{E}_{it} f_t(k). \end{aligned} \quad (61)$$

Remark 5. This section provides a scheme for determining the subsystem that suffers from a fault, and N observers are designed. If $\bar{f}_t(k) = 0$, the t -th subsystem suffers from a fault; if there exists a fault in another subsystem, $\bar{f}_t(k) = 0$.

The following theorem is presented to facilitate the design method. There exist matrices such that the design condition can be guaranteed.

Theorem 4. For any $i \neq j$, $0 < \lambda_1 < 1$, $\lambda_2 > 1$, there exist matrices \bar{G}_{it} , \bar{K} , symmetric positive definite matrices $\bar{P}_{\eta i} = \bar{P}_{\eta i}^T > 0$, $\bar{P}_{\eta j} = \bar{P}_{\eta j}^T > 0$, $\bar{P}_{fi} = \bar{P}_{fi}^T > 0$, $\bar{P}_{fj} = \bar{P}_{fj}^T > 0$, $\bar{Q}_{fi} = \bar{Q}_{fi}^T > 0$, and scalars a_5 , a_6 , a_7 , and a_8 such that following inequalities hold:

$$\bar{P}_{\eta i} < \lambda_2 \bar{P}_{\eta j}, \quad \bar{P}_{fi} < \lambda_2 \bar{P}_{fj}, \quad (62)$$

$$\begin{bmatrix} -\lambda_1 \bar{P}_{\eta i} + a_5 \text{He}\{\bar{G}_{it}\bar{T}_{it}\bar{A}_{it} + \bar{W}_{it}\bar{C}_{it}\} & -a_5 \bar{G}_{it} + \bar{A}_{it}^T \bar{T}_{it}^T \bar{G}_{it}^T + \bar{C}_{it}^T \bar{W}_{it}^T \\ * & \bar{P}_{\eta i} - \bar{G}_{it} - \bar{G}_{it}^T \end{bmatrix} < 0, \quad (63)$$

$$\begin{bmatrix} \Omega_{11} & \Omega_{12} & \Omega_{13} \\ * & \Omega_{22} & \Omega_{23} \\ * & * & \Omega_{33} \end{bmatrix} < 0, \quad (64)$$

$$\begin{bmatrix} -\bar{P}_{\eta i} & \bar{C}_{it}^T \\ \bar{C}_{it} & -\frac{1}{b}I \end{bmatrix} < 0, \quad (65)$$

$$\begin{bmatrix} -\lambda_1 \bar{P}_{fi} + a_7 \text{He}\{\bar{G}_{it} \bar{T}_{it} \bar{A}_{it} + \bar{W}_{it} \bar{C}_{it}\} & -a_7 \bar{G}_{it} + \bar{A}_{it}^T \bar{T}_{it}^T \bar{G}_{it}^T + \bar{C}_{it}^T \bar{W}_{it}^T \\ * & P_{fi} - \bar{G}_{it} - \bar{G}_{it}^T \end{bmatrix} < 0, \quad (66)$$

$$\begin{bmatrix} \Pi_{11} & \Pi_{12} & \Pi_{13} \\ * & \Pi_{22} & \Pi_{23} \\ * & * & \Pi_{33} \end{bmatrix} < 0, \quad (67)$$

$$\begin{cases} \Omega_{11} = -\bar{P}_{\eta i} + (1-b)\bar{C}_{it}^T \bar{C}_{it} + \text{He}\{a_6(\bar{G}_{it} \bar{T}_{it} \bar{A}_{it} + \bar{W}_{it} \bar{C}_{it})\}, \\ \Omega_{12} = a_6 \bar{G}_{it} \bar{T}_{it} \bar{D}_i, \\ \Omega_{13} = -a_6 \bar{G}_{it} + \bar{A}_{it}^T \bar{T}_{it}^T \bar{G}_{it}^T + \bar{C}_{it}^T \bar{W}_{it}^T, \\ \Omega_{22} = -\bar{\mu}^2 I, \\ \Omega_{23} = \bar{D}_i^T \bar{T}_{it}^T \bar{G}_{it}^T, \\ \Omega_{33} = \bar{P}_{\eta i} - \bar{G}_{it} - \bar{G}_{it}^T, \end{cases}$$

$$\begin{cases} \Pi_{11} = -\lambda_1 \bar{P}_{fi} - 2 \cos(\omega_l) \bar{Q}_{fi} - \bar{C}_{it}^T \bar{C}_{it} + \text{He}\{a_8(\bar{G}_{it} \bar{T}_{it} \bar{A}_{it} + \bar{W}_{it} \bar{C}_{it})\}, \\ \Pi_{12} = (\bar{A}_{it}^T \bar{T}_{it}^T \bar{G}_{it}^T + \bar{C}_{it}^T \bar{W}_{it}^T) \bar{K} + a_8 \bar{G}_{it} \bar{T}_{it} \mathcal{E}_{it}, \\ \Pi_{13} = -a_8 \bar{G}_{it} + \bar{Q}_{fi} + \bar{A}_{it}^T \bar{T}_{it}^T \bar{G}_{it}^T + \bar{C}_{it}^T \bar{W}_{it}^T, \\ \Pi_{22} = \bar{\beta}^2 I + \text{He}\{\bar{K}^T \bar{G}_{it} \bar{T}_{it} \mathcal{E}_{it}\}, \\ \Pi_{23} = \mathcal{E}_{it}^T \bar{T}_{it}^T \bar{G}_{it}^T - \bar{K}^T \bar{G}_{it}, \\ \Pi_{33} = \bar{P}_{fi} - \bar{G}_{it} - \bar{G}_{it}^T. \end{cases}$$

Proof. After \bar{W}_{it} and \bar{G}_{it} are obtained, matrix \bar{L}_{it} is calculated by $\bar{L}_{it} = \bar{G}_{it}^{-1} \bar{W}_{it}$. The proof is obtained by the similar approaches to those of Theorem 3 and is omitted here.

The following optimization problem is solved:

$$\min \bar{\mu} + \bar{\beta} \quad \text{s.t. Eqs. (62)–(67)}.$$

4.2 Isolation scheme

To discuss which subsystem has the fault, residual evaluation functions are determined as $J_r = \|\bar{r}(k)\|$ and $J_{rt} = \|\bar{r}_t(k)\|$. The corresponding threshold J_{th} is chosen as $J_{th} = \sup_{f(k)=0} J_r$ when the system has no fault.

The isolation scheme gives the alarm rule by adopting the following detection logic that compares the evaluation function of the t -th subsystem with the corresponding threshold. The logic is adopted as

$$\begin{cases} J_{rt} \leq J_{th} \Rightarrow \text{the } t\text{-th system with no alarm,} \\ J_{rt} > J_{th} \Rightarrow \text{the } t\text{-th system with alarm.} \end{cases}$$

We determine that the t -th subsystem suffers from the fault when the residual exceeds the threshold, i.e., $J_{rt} > J_{th}$, and the t -th subsystem has no fault when $J_{rt} \leq J_{th}$.

5 Simulation examples

5.1 System model

In this subsection, the traffic density model [52, 53] is used to prove the feasibility of the proposed method. We assume that l cells are involved in a link. The connection relationship between links is shown in Figure 1, and we obtain the dynamic equation of each cell. The dynamic of a link is proposed as (1), and the traffic density vector is defined as $x_t(k) = [x_{t1}, \dots, x_{tn_x}]$. The entire urban freeway network

is designed as (2), where $x(k) = [x_1^T(k), \dots, x_N^T(k)]$ and $u(k) = [u_1^T(k), \dots, u_N^T(k)]$ are the traffic density vector and the traffic demand of the interconnected system, respectively.

Several model parameters of the switched system are provided as

$$\begin{aligned}
 A_1 &= \begin{bmatrix} -0.5 & 0 & 0 \\ 0.6 & -0.2 & 0.1 \\ 0 & 0.2 & -0.2 \end{bmatrix}, \quad B_1 = \begin{bmatrix} -0.3 \\ 0.25 \\ 0 \end{bmatrix}, \quad D_1 = \begin{bmatrix} -0.3 \\ 0.4 \\ -0.5 \end{bmatrix}, \\
 A_2 &= \begin{bmatrix} -0.4 & 0.2 & 0 \\ 0 & -0.4 & 0.2 \\ 0.2 & 0 & -0.2 \end{bmatrix}, \quad B_2 = \begin{bmatrix} 0 \\ 0.5 \\ 1.5 \end{bmatrix}, \quad D_2 = \begin{bmatrix} -0.2 \\ 0.3 \\ -0.3 \end{bmatrix}, \\
 C_1 = C_2 &= \begin{bmatrix} 0.4 & 0 & 0 \\ 0 & -0.4 & -0.4 \end{bmatrix}, \quad \Lambda = \begin{bmatrix} 0.5 & 0 \\ 0 & 0.5 \\ 0 & 0 \end{bmatrix}, \\
 \mathcal{G} &= \begin{bmatrix} 2 & -1 & -1 & 0 \\ -1 & 3 & -1 & -1 \\ -1 & -1 & 3 & -1 \\ 0 & -1 & -1 & 2 \end{bmatrix}.
 \end{aligned}$$

On the basis of (11), let $\lambda_1 = 0.6$ and $\lambda_2 = 2.5$, and we can determine that $\tau^* = 1.7937$. Hence, $\tau = 2$, and Figure 2 shows the switching signal.

Let

$$u(k) = \begin{cases} 3\cos(0.3k) + 1.6k < 80, \\ 3.6\sin(0.5k)k \geq 80, \end{cases}$$

and the disturbance $\eta_t(k)$ is proposed as

$$\eta_t(k) = \begin{cases} 0.035k < 150, \\ 0.06k \geq 150. \end{cases}$$

Several parameters are given as $a = 0.1$, $b = 0.4$, $a_1 = -0.5$, $a_2 = -0.4$, $a_3 = -0.75$, $a_4 = -0.8$, $a_5 = 0.6$, $a_6 = -0.73$, $a_7 = -0.7$, and $a_8 = 0.65$, and matrices are provided as

$$K = -5 \times \begin{bmatrix} 0.5 & 0.4 & 0.5 & 0.5 & 0.4 & 0.5 & 0.5 & 0.4 & 0.5 & 0.5 & 0.4 & 0.5 \\ 1 & 0.5 & 0.45 & 1 & 0.5 & 0.45 & 1 & 0.5 & 0.45 & 1 & 0.5 & 0.45 \\ 1 & 0.4 & 0.3 & 1 & 0.4 & 0.3 & 1 & 0.4 & 0.3 & 1 & 0.4 & 0.3 \\ 0.5 & 1 & 0.3 & 0.5 & 1 & 0.3 & 0.5 & 1 & 0.3 & 0.5 & 1 & 0.3 \end{bmatrix}^T,$$

$$\bar{K} = -0.5 \times [2 \ 3 \ 4 \ 4 \ 2.5 \ 1 \ 1 \ 2 \ 1 \ 1 \ 2 \ 2.5 \ 3 \ 2 \ 3],$$

and

$$Z_1 = Z_2 = [0_{12 \times 8} \ I_{12}], \quad \bar{Z}_{11} = \bar{Z}_{21} = \bar{Z}_{14} = \bar{Z}_{24} = 0.05 \times [0_{15 \times 5} \ I_{15}].$$

5.2 State estimation and fault detection

(1) Assume that $f(k) = 0$, and initial values are proposed as

$$x_0 = [1 \ 2.5 \ 1.4 \ 1.6 \ 2.5 \ 2 \ 1.4 \ 2 \ 1.5 \ 1.4 \ 1.6 \ 2]^T,$$

$$\hat{x}_0 = -1 \times [3.5 \ 1.75 \ 2.25 \ 1.75 \ 3 \ 3.5 \ 3.5 \ 1.75 \ 2.25 \ 1.75 \ 3 \ 3.5]^T.$$

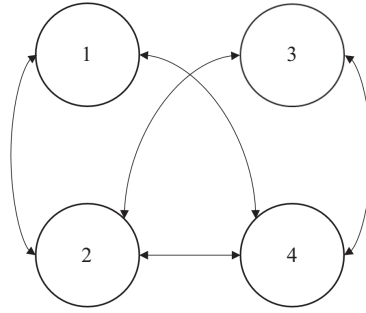


Figure 1 Topology of the system.

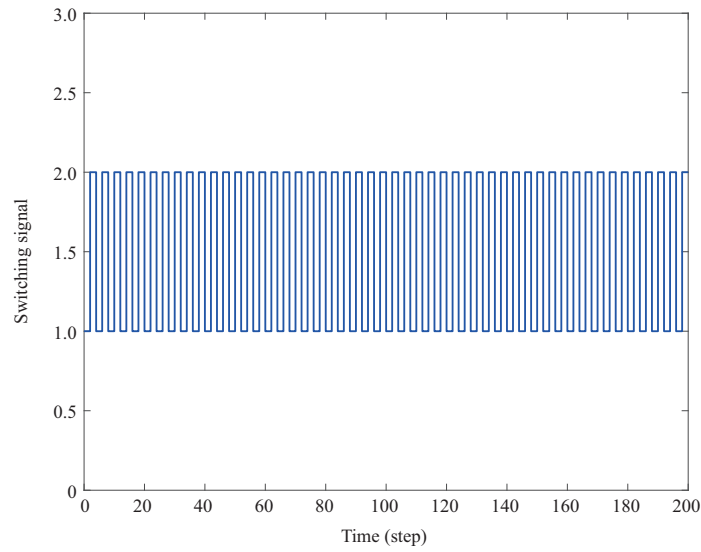


Figure 2 (Color online) Switching signal.

The simulation results are depicted in Figures 3(a)–(d), where the solid lines denote the actual states, and the dashed lines denote the estimation states. Clearly, the estimation performance of the provided method is guaranteed for a system with unknown input.

(2) Assume that the frequency range of $f(k)$ satisfies $|\omega| \leq 0.2$, and the values of $f(k)$ are chosen as $f_2(k) = f_3(k)$,

$$f_1(k) = \begin{cases} 0.5, & k < 150, \\ 0, & \text{else,} \end{cases} \quad f_4(k) = \begin{cases} 0.35, & 50 < k < 100, \\ 0, & \text{else.} \end{cases}$$

Consider that $x(k) = \hat{x}(k) = 0$. Figure 4 shows the detection results, where the solid line denotes the residual signal generated by the proposed method, and the dashed line denotes the threshold. The dotted line denotes the residual generated by the method using H_∞ in [36]. When $k > 150$ and $50 < k < 100$, the residuals generated by both methods can exceed the threshold. On the basis of the proposed detection strategy, the system is clearly affected by faults. According to Figure 4, the proposed method generates the residual with a larger value, making the residuals more sensitive than those of the method using H_∞ .

5.3 Fault isolation

According to the above section, faults are detected when $k > 150$ and $50 < k < 100$ without knowing which subsystem has a fault signal. Figures 5(a)–(d) show the relationship between the residual signals and the threshold. Figures 5(a) and (d) clearly show that J_{rt} exceeds the threshold when $k > 150$ in subsystem 1, and J_{rt} exceeds the threshold when $50 < k < 100$ in subsystem 4. The solid lines denote J_{rt} generated by the proposed method, and the dashed lines denote the threshold. Figures 5(b) and (c) show that all residuals of subsystems 2 and 3 always fall below the thresholds, while those of subsystems 1

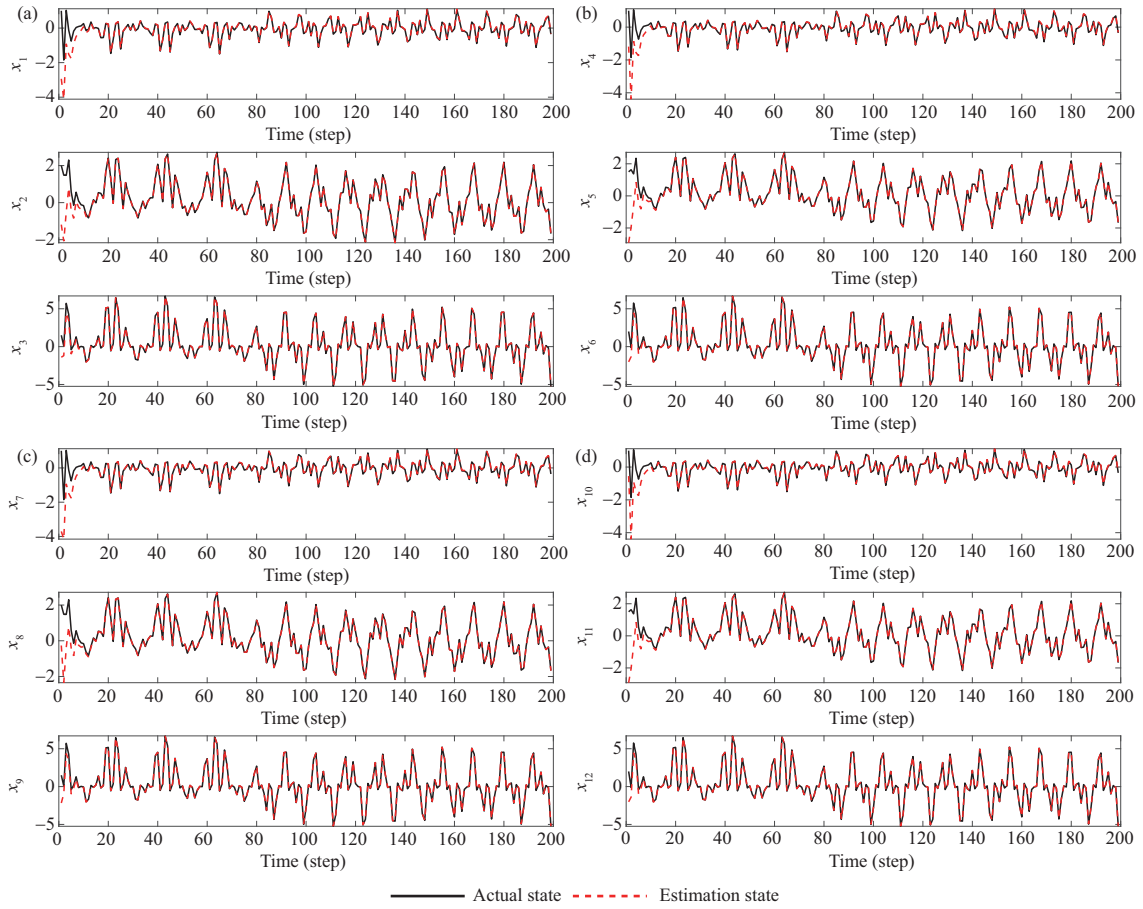


Figure 3 (Color online) State estimation of (a) subsystem 1, (b) subsystem 2, (c) subsystem 3, and (d) subsystem 4.

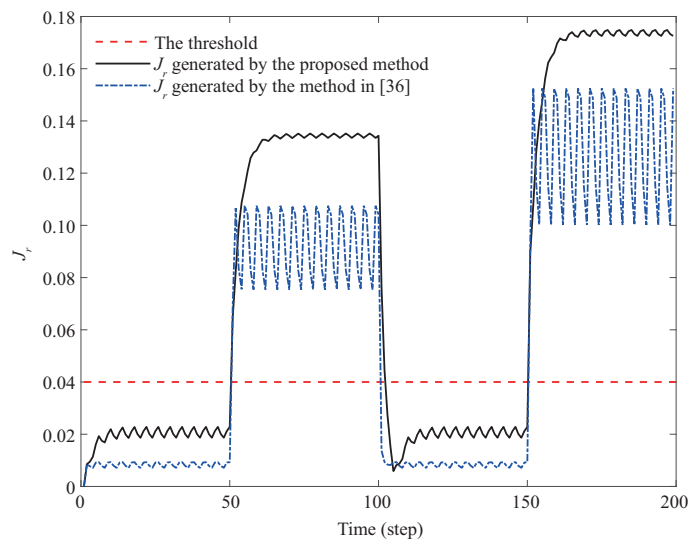


Figure 4 (Color online) Residuals and the generated threshold.

and 4 can exceed the threshold quickly after the fault signal. In conclusion, the fault is imposed on subsystems 1 and 4, respectively.

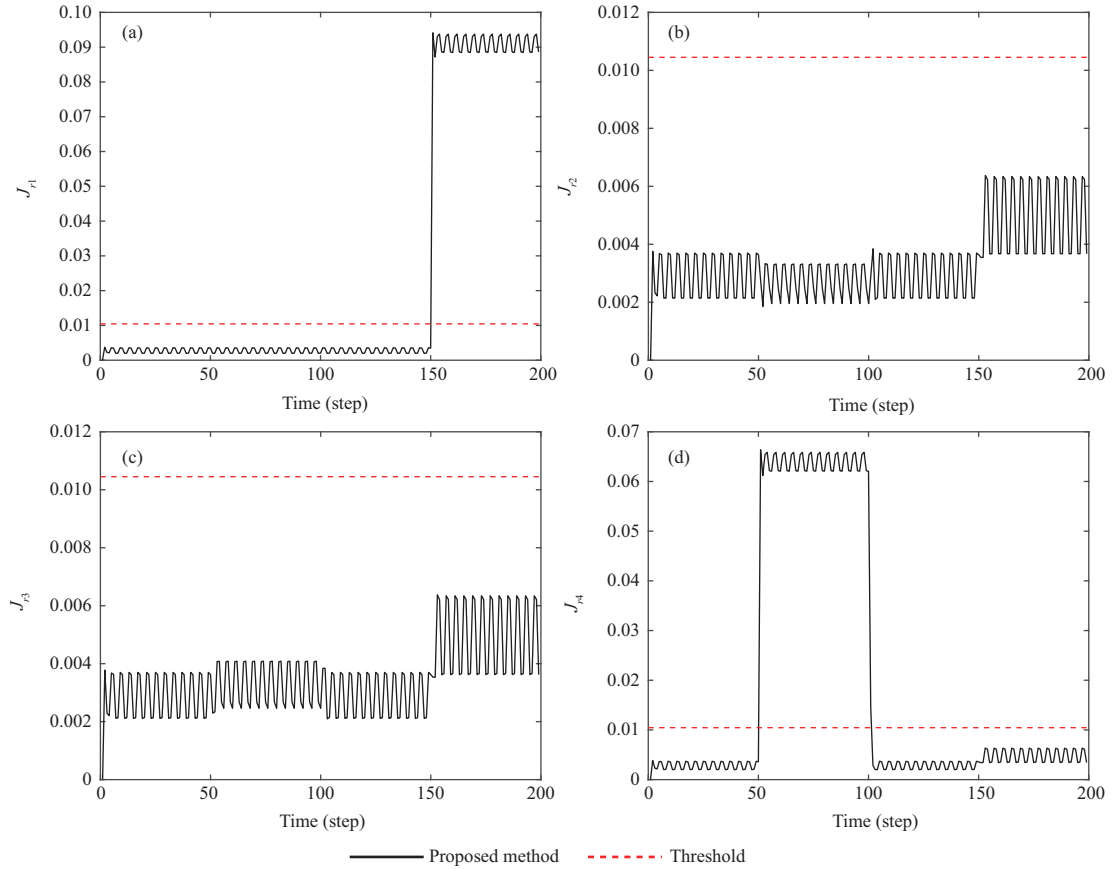


Figure 5 (Color online) Residuals and generated thresholds of (a) subsystem 1, (b) subsystem 2, (c) subsystem 3, and (d) subsystem 4.

6 Conclusion

In this paper, the problem of FDI for the switched CPS is addressed, and the ADT method is adopted to guarantee stability analysis. Assuming that faults belong to a low-frequency range, the observer is designed to guarantee that the generated residual is sensitive to faults and robust against unknown bounded disturbances. Based on the proposed detector, an isolation strategy is provided by comparing the t -th generated residual with the threshold. The simulation results finally demonstrated the effectiveness of the proposed method. Compared with the method using the H_∞ technique, the proposed detection method is obviously more sensitive to faults.

Acknowledgements This work was supported in part by National Natural Science Foundation of China (Grant Nos. 62273065, 61703296), China Postdoctoral Science Foundation (Grant No. 2022M721901), and Opening Project of the Key Laboratory of Bionic Engineering (Ministry of Education), Jilin University (Grant No. K202208).

References

- Huang R, Zhang J H, Zhang X. Adaptive tracking control of uncertain switched non-linear systems with application to aircraft wing rock. *IET Control Theory Appl*, 2016, 10: 1755–1762
- Shen H, Xing M P, Wu Z G, et al. Multiobjective fault-tolerant control for fuzzy switched systems with persistent dwell time and its application in electric circuits. *IEEE Trans Fuzzy Syst*, 2020, 28: 2335–2347
- Elliott R, Sun P Y, Zhu T. Electricity prices and industry switching: evidence from Chinese manufacturing firms. *Energy Economics*, 2019, 78: 567–588
- Guo Y X, Ge S S, Fu J T, et al. Stability and stabilization of a class of switched stochastic systems with saturation control. *Sci China Inf Sci*, 2021, 64: 222201
- Ren H L, Zong G D, Karimi H R. Asynchronous finite-time filtering of networked switched systems and its application: an event-driven method. *IEEE Trans Circuits Syst I*, 2019, 66: 391–402
- Mu X W, Hu Z H. Stability analysis for semi-Markovian switched stochastic systems with asynchronously impulsive jumps. *Sci China Inf Sci*, 2021, 64: 112206

- 7 Aazan G, Girard A, Greco L, et al. Stability of shuffled switched linear systems: a joint spectral radius approach. *Automatica*, 2022, 143: 110434
- 8 Yang H, Zhao X D, Jiang B. Stability analysis of switched positive nonlinear systems: an invariant ray approach. *Sci China Inf Sci*, 2019, 62: 212206
- 9 Taousser F Z, Djouadi S M, Tomsovic K. A dwell time approach for the stabilization of mixed continuous/discrete switched systems. *Automatica*, 2022, 142: 110386
- 10 Zhang S Y, Nie H. Dwell-time-dependent asynchronous mixed H_∞ and passive control for discrete-time switched systems. *Nonlinear Anal-Hybrid Syst*, 2022, 44: 101140
- 11 Zhuang S L, Yu X H, Qiu J B, et al. Meta-sequence-dependent H_∞ filtering for switched linear systems under persistent dwell-time constraint. *Automatica*, 2021, 123: 109348
- 12 Li Y, Zhang H B. Stability, L_1 -gain analysis and asynchronous L_1 -gain control of uncertain discrete-time switched positive linear systems with dwell time. *J Franklin Institute*, 2019, 356: 382–406
- 13 Lu A Y, Yang G H. Stabilization of switched systems with all modes unstable via periodical switching laws. *Automatica*, 2020, 122: 109150
- 14 Ma R C, An S, Fu J. Dwell-time-based stabilization of switched positive systems with only unstable subsystems. *Sci China Inf Sci*, 2021, 64: 119205
- 15 Yang R N, Zheng W X. H_∞ filtering for discrete-time 2-D switched systems: an extended average dwell time approach. *Automatica*, 2018, 98: 302–313
- 16 Yu Q, Lv H. Stability analysis for discrete-time switched systems with stable and unstable modes based on a weighted average dwell time approach. *Nonlinear Anal-Hybrid Syst*, 2020, 38: 100949
- 17 Qi W H, Park J H, Cheng J, et al. Exponential stability and L_1 -gain analysis for positive time-delay Markovian jump systems with switching transition rates subject to average dwell time. *Inf Sci*, 2018, 424: 224–234
- 18 Liu L J, Zhao X D, Sun X M, et al. Stability and l_2 -gain analysis of discrete-time switched systems with mode-dependent average dwell time. *IEEE Trans Syst Man Cybern Syst*, 2020, 50: 2305–2314
- 19 Huang D R, Hua X X, Mi B, et al. Incipient fault diagnosis on active disturbance rejection control. *Sci China Inf Sci*, 2022, 65: 199202
- 20 Guo S H, Zhu F L, Jiang B. Reduced-order switched UIO design for switched discrete-time descriptor systems. *Nonlinear Anal-Hybrid Syst*, 2018, 30: 240–255
- 21 Hua X X, Huang D R, Guo S H. Extended state observer based on ADRC of linear system with incipient fault. *Int J Control Autom Syst*, 2020, 18: 1425–1434
- 22 Huang J, Ma X, Che H C, et al. Further result on interval observer design for discrete-time switched systems and application to circuit systems. *IEEE Trans Circuits Syst II*, 2020, 67: 2542–2546
- 23 Choi H D, Ahn C K, Karimi H R, et al. Filtering of discrete-time switched neural networks ensuring exponential dissipative and $l_2 - l_\infty$ performances. *IEEE Trans Cybern*, 2017, 47: 3195–3207
- 24 Xiong S X, Wu Q X, Wang Y H, et al. An $l_2 - l_\infty$ distributed containment coordination tracking of heterogeneous multi-unmanned systems with switching directed topology. *Appl Math Computation*, 2021, 404: 126080
- 25 Du D X, Yang Y, Zhao H, et al. Robust fault diagnosis observer design for uncertain switched systems. *Int J Control Autom Syst*, 2020, 18: 3159–3166
- 26 Mei Z, Fang T, Shen H. Finite-time $l_2 - l_\infty$ filtering for persistent dwelltime switched piecewise-affine systems against deception attacks. *Appl Math Computation*, 2022, 427: 127088
- 27 Hu X H, Xia J W, Chen X Y, et al. Non-fragile $l_2 - l_\infty$ synchronization for switched inertial neural networks with random gain fluctuations: a persistent dwell-time switching law. *Neurocomputing*, 2020, 403: 193–202
- 28 Tai W P, Zuo D D, Xuan Z X, et al. Non-fragile $l_2 - l_\infty$ filtering for a class of switched neural networks. *Math Comput Simul*, 2021, 185: 629–645
- 29 Hou L L, Zhao X D, Sun H B, et al. $l_2 - l_\infty$ filtering of discrete-time switched systems via admissible edge-dependent switching signals. *Syst Control Lett*, 2018, 113: 17–26
- 30 Xiang W M, Lam J, Li P S. On stability and H_∞ control of switched systems with random switching signals. *Automatica*, 2018, 95: 419–425
- 31 Chen Y, Zhu M Z, Lu R Q, et al. Distributed H_∞ filtering of nonlinear systems with random topology by an event-triggered protocol. *Sci China Inf Sci*, 2021, 64: 202204
- 32 Shen Y X, Wang Z D, Shen B, et al. H_∞ state estimation for multi-rate artificial neural networks with integral measurements: a switched system approach. *Inf Sci*, 2020, 539: 434–446
- 33 Zhang H, Wang Z P, Yan H C, et al. Adaptive event-triggered transmission scheme and H_∞ filtering co-design over a filtering network with switching topology. *IEEE Trans Cybern*, 2019, 49: 4296–4307
- 34 Gao H, Shi K B, Zhang H B. A novel event-triggered strategy for networked switched control systems. *J Franklin Institute*, 2021, 358: 251–267
- 35 Liu X X, Su X J, Shi P, et al. Fault detection filtering for nonlinear switched systems via event-triggered communication approach. *Automatica*, 2019, 101: 365–376

- 36 Li J, Pan K P, Zhang D Z, et al. Robust fault detection and estimation observer design for switched systems. *Nonlinear Anal-Hybrid Syst*, 2019, 34: 30–42
- 37 Su Q Y, Fan Z X, Lu T, et al. Fault detection for switched systems with all modes unstable based on interval observer. *Inf Sci*, 2020, 517: 167–182
- 38 Zhai D, Lu A Y, Li J H, et al. Simultaneous fault detection and control for switched linear systems with mode-dependent average dwell-time. *Appl Math Computation*, 2016, 273: 767–792
- 39 Zhang Z H, Yang G H. Interval observer-based fault isolation for discrete-time fuzzy interconnected systems with unknown interconnections. *IEEE Trans Cybern*, 2017, 47: 2413–2424
- 40 Zhu F L, Tang Y Y, Wang Z H. Interval-observer-based fault detection and isolation design for T-S fuzzy system based on zonotope analysis. *IEEE Trans Fuzzy Syst*, 2022, 30: 945–955
- 41 Zammali C, Wang Z H, Gorp J V, et al. Fault detection for switched systems based on pole assignment and zonotopic residual evaluation. *IFAC-PapersOnLine*, 2020, 53: 4695–4700
- 42 Wang H M, Yang G H, Ye D. Fault detection and isolation for affine fuzzy systems with sensor faults. *IEEE Trans Fuzzy Syst*, 2016, 24: 1058–1071
- 43 Zhou M, Rodrigues M, Shen Y, et al. H_-/H_∞ fault detection observer design for a polytopic LPV system using the relative degree. *Int J Appl Math Comput Sci*, 2018, 28: 83–95
- 44 Liao F, Zhu Y Z, Yang R N, et al. Integrated fault estimation and tolerant control for discrete-time switched affine systems with mixed switching laws. *Nonlinear Anal-Hybrid Syst*, 2022, 44: 101167
- 45 Zhang X Y. Robust integral sliding mode control for uncertain switched systems under arbitrary switching rules. *Nonlinear Anal-Hybrid Syst*, 2020, 37: 100900
- 46 Wang X H, Tan C P, Zhou D H. A novel sliding mode observer for state and fault estimation in systems not satisfying matching and minimum phase conditions. *Automatica*, 2017, 79: 290–295
- 47 Zhu F L. State estimation and unknown input reconstruction via both reduced-order and high-order sliding mode observers. *J Process Control*, 2012, 22: 296–302
- 48 Zhang J C, Zhao X D, Zhu F L, et al. Reduced-order observer design for switched descriptor systems with unknown inputs. *IEEE Trans Automat Contr*, 2020, 65: 287–294
- 49 Zhang X M, Zhu F L. Observer-based sensor attack diagnosis for cyber-physical systems via zonotope theory. *Asian J Control*, 2021, 23: 2444–2458
- 50 Liang D G, Yang Y, Li R C, et al. Finite-frequency H_-/H_∞ unknown input observer-based distributed fault detection for multi-agent systems. *J Franklin Institute*, 2021, 358: 3258–3275
- 51 Wang H, Yang G H. A finite frequency domain approach to fault detection observer design for linear continuous-time systems. *Asian J Control*, 2008, 10: 559–568
- 52 Guo Y Q. Dynamic-model-based switched proportional-integral state observer design and traffic density estimation for urban freeway. *Eur J Control*, 2018, 44: 103–113
- 53 Zeroual A, Harrou F, Sun Y. Road traffic density estimation and congestion detection with a hybrid observer-based strategy. *Sustain Cities Soc*, 2019, 46: 101411